PHYSICAL REVIEW B VOLUME 17, NUMBER 8 15 APRIL 1978

Transport studies near phase transitions in $NbSe_3$

N. P. Ong
Department of Physics, University of Southern California, Los Angeles, California 90007
(Received 8 August 1977)

The non-Ohmic transport properties of $NbSe_3$ are studied near the two phase transitions at T_1 and T_2. From the non-Ohmic data a parameter α is obtained which provides information on the fraction of Fermi surface affected by the phase transitions. By relating α to a BCS-type gap and modifying the calculations of Fedders and Martin on the spin-density-wave state in Cr we have obtained a theoretical curve for α which agrees well with the experimental data. This good agreement provides new indirect evidence for the charge-density-wave (CDW) state in $NbSe_3$. The derivative of the low-field resistivity versus temperature has also been measured and is shown to be divergent at T_1 and T_2. The index of this divergence is presented and its significance to the dimensionality of the system is discussed. Finally, we briefly discuss the possibility of explaining the non-Ohmicity below T_1 in terms of nonlinear excitations in a CDW condensate.

I. INTRODUCTION

The transition-metal trichalcogenide[1-3] $NbSe_3$ undergoes two phase transitions at the temperatures T_1 (142 K) and T_2 (58 K). The electronic conductivity is greatly perturbed by processes which set in at T_1 and T_2, as evidenced by the appearance of two giant anomalies in the resistivity. The conductivity within these anomalies has been shown[3,4] to be highly non-Ohmic, with the conductivity increasing rapidly as the applied electric field is increased. The frequency dependence of the conductivity is also anomalous.[3] At a frequency of 9 GHz, no evidence of the T_2 transition appears in the microwave resistivity while the T_1 anomaly is sharply reduced in size compared to the dc case. In conjunction with other indirect experimental evidence which will be discussed in Sec. IV A, the two transitions have been tentatively identified with the formation of charge-density waves (CDW's). If this hypothesis is valid, the non-Ohmic behavior and the anomalous frequency dependence raise the intriguing possibility that nonlinear excitations are being observed in a CDW condensate. Such excitations have been the subject of much theoretical discussion. In particular, Rice, Bishop, Krumhansl and Trullinger[5] have described the excitation of solitonlike ϕ particles in a one-dimensional (1D) CDW system. Maki[6] has also discussed the electric-field generation of solitons as a possible source of non-Ohmicity. The lack of direct experimental evidence (from x-ray or neutron scattering) for superlattice formation in $NbSe_3$ makes the CDW model rather provisional and it is entirely possible that the phase transitions are caused by a different instability. (See note added in proof.) However, all experimental evidence obtained to date is consistent with the CDW model and recent Hall-effect measurements[7] have provided direct evidence of a large loss of carriers at both T_1 and T_2. This is to be expected from a theory in which sections of the Fermi surface (FS) are destroyed by gap formation.

In this paper the behavior near T_1 and T_2 of the various parameters associated with the non-Ohmicity are presented and the results are analyzed using a model in which a fraction of the carriers are removed by gap formation at the FS. The temperature dependence of the parameter α [defined in Eq. (2)] is interpreted in terms of thermal excitations of carriers across a growing gap. An equation is derived relating α to the gap function Δ and good agreement between experiment and theory is obtained, using appropriately scaled Bardeen-Cooper-Schrieffer (BCS)[8] values for the gap Δ. To obtain the transition temperatures, the derivative of the low-electric-field resistivity with respect to temperature has been measured and shown to diverge at the two transitions. The critical index of this divergence provides an indication of the conductivity anisotropy but the conclusions are not firmly established because of the rounding off of the divergence very near T_1 and T_2 in the present data.

Below T_1 and T_2, the non-Ohmicity of the conductivity obeys the equation[3]

$$\sigma(E,T)=\sigma_{an}(T)+\sigma_{bn}(T)e^{-E_{0n}/E}, n=1,2, \quad (1)$$

where E is the applied electric field, T is the temperature, and the subscripts 1 and 2 identify the transitions. The activation field E_{0n} is strongly temperature dependent. Its temperature dependence as well as that of σ_a and σ_b have been described in Ref. 3, where the parameter α_n defined by

$$\alpha_n=\sigma_{bn}/(\sigma_{an}+\sigma_{bn}), \quad n=1,2 \quad (2)$$

was introduced. Arguing from the fact that the conductivity is proportional to the FS area we in-

terpreted[3] α_n as measuring the fraction of FS destroyed by gap formation. α_n was shown to grow from zero at T_n and saturate to a constant value at temperatures below that at which the low-field resistivity peaks. However, insofar as the above interpretation of α_n is not unique, we shall discuss a slightly different interpretation of α_n here. The new interpretation considers the α_n (suitably normalized) to measure the number of carriers thermally excited across a growing gap. As opposed to the interpretation in Ref. 3, the fraction of FS destroyed by gap formation is considered to be temperature independent. The loss of carriers is still a smooth function of temperatures because the size of the gap increases smoothly from zero, and thermal excitation of carriers across this gap decreases in relation to the size of the gap.

II. EXPERIMENTAL

All the measurements were done in the four-probe configuration with the leads attached to the sample by silver paint. The non-Ohmic data were taken using pulsed currents with a pulse width of 2 μsec and a duty cycle of 10^{-4}. Typically the maximum power dissipation across a sample of 30 Ω was 5×10^{-7}W. This was inferred to be well within the thermal capacity of the cryogenic system because a dc current dissipating the same power in the sample revealed no signs of temperature increase in the sample. Pulse heights were measured by means of a bucking variable-voltage reference as described in Ref. 3. The uncertainty and reproducibility of the measurements were 1 in 10^3, decreasing to 1 in 10^2 for the smallest pulses. To ensure that there was no hysteresis in the measured conductivity (as the E field was varied at a fixed temperature) dc measurements using a 10-μA current were performed before and after each pulse measurement. In samples which were inadvertently damaged by excessively heavy pulses (typically 25 mA into a 30-Ω sample) the measured conductivity showed large hysteresis and was not reproducible. Microscopic examination of these damaged samples invariably showed the presence of broken strands which separate from the main body of the sample. For undamaged samples no hysteresis under field variation or thermal cycling was observed to the accuracy of the measurements and results were reproducible after a warm-up to room temperature and subsequent cool down. The temperature was measured by a calibrated silicon diode sensor and the stability was maintained to ±20 mK for the 20 min required to complete the non-Ohmic measurement at each temperature point.

In the measurements of the low-field-resistivity derivative the temperature was allowed to drift at a rate of 0.1 K/min pass the transitions, and the voltage across the sample was measured in 70-mK steps with an HP standard differential voltmeter. The derivative was computed by differentiating the best quadratic fit to the resistance at five adjacent temperature points. There was a hysteresis of approximately 0.1 K between cooling and warming runs, but the two transitions were inferred to be second order because the displacement between cooling and warming curves was temperature independent to ±20 mK.

III. RESULTS

From Eq. (1) we have the conductivity in the two limits of weak and strong fields

$$\sigma(E\to 0)=\sigma_{an}, \tag{3}$$

$$\sigma(E\to\infty)=\sigma_{an}+\sigma_{bn}. \tag{4}$$

In Eq. (3), σ_{an} is just the low-field conductivity. If Eq. (1) is valid then by plotting $\ln(\sigma-\sigma_a)$ vs $1/E$, we should obtain a straight line. From the slope and intercept of this straight line the values of E_0 and σ_{bn} may be obtained. The parameter α_n is then computed from Eq. (2). In Ref. 3 preliminary measurements showed α_n to increase from zero at T_n and then saturate to a temperature-independent value at lower temperatures. E_{0n} appears to attain a large value just below T_n, decrease to a minimum, and then increase rapidly as the temperature is lowered. In this paper more extensive data on α_n and E_{0n} are reported, in particular near T_1 and T_2. Figure 1 shows α_2 and E_{02} at temperatures near T_2. α_2 (solid circles) grows smoothly from zero as $(T_2-T)^{1/2}$ close to T_2. The solid line obeys the equation $2.05\,(1-T/T_2)^{1/2}$. At lower temperatures, the experimental points deviate from the solid line. This behavior, reminiscent of the behavior of the gap function Δ in the BCS theory of superconductivity, has prompted us to relate α_n to Δ. This will be discussed in Sec. IV B. The open circles represent the measured activation field E_{02}. It may be seen to diverge as T approaches T_2^-. The source of this divergence is still unclear. The broken line indicates the low-field resistivity ρ (zero suppressed). It may be seen that deviation from the pretransition linear behavior occurs 2 K above T_2. This is ascribed to scattering from fluctuations in the gap in analogy to the case in itinerant antiferromagnets (see Sec. IV D). Figure 2 displays the same quantities α_1 and E_{01} close to the T_1 transition. The larger error bars reflect the greater uncertainty in the measurements caused by the smaller change in σ induced by a given field. (The activation field near T_1 is about an order of magnitude larger than that near T_2

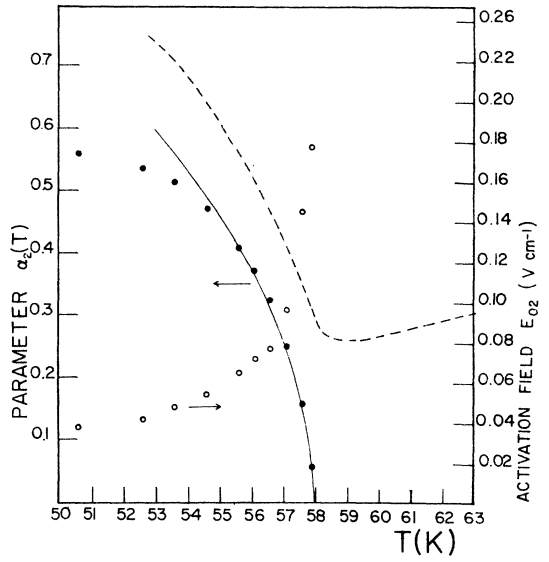

FIG. 1. Behavior of the parameter α_2 (solid circles) and activation field E_{02} (open circles) near T_2. The solid line is the mean-field prediction of the temperature dependence $(T_c - T)^{1/2}$. The broken line is the low-field resistivity (zero suppressed).

while the maximum relative increase in σ is three times smaller near T_1.) Nevertheless, behavior similar to that of α_2 and E_{02} is obtained for α_1 and E_{01}. The solid line has the equation $0.849(1 - T/T_1)^{1/2}$.

In Figs. 3 and 4 the critical behavior of α_n and

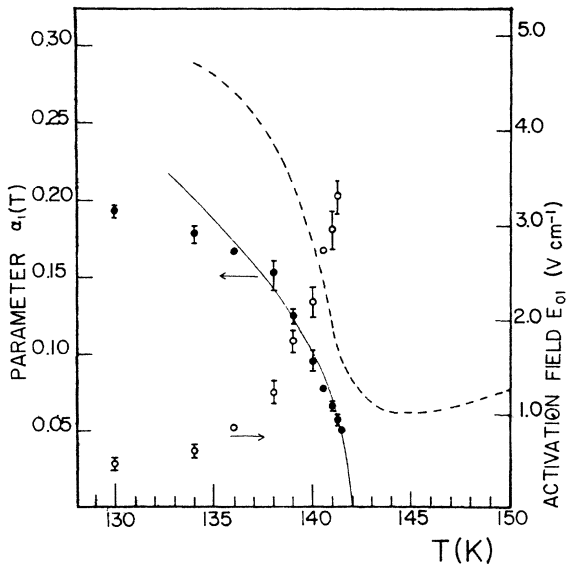

FIG. 2. Behavior of the parameter α_1 (solid circles) and activation field E_{01} (open circles) near T_1. The solid line is mean-field behavior. The broken line is the low-field resistivity with zero suppressed.

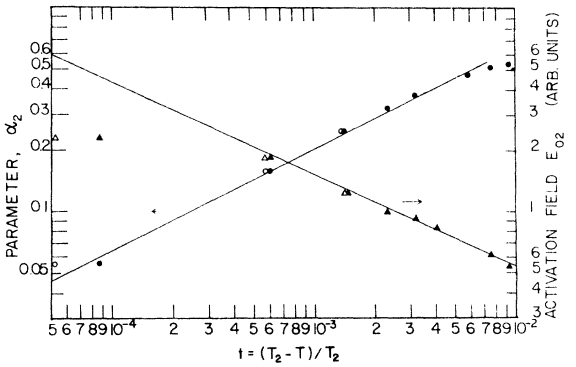

FIG. 3. Log-log plot of α_2 (circles) and E_{02} (triangles) versus the reduced temperature $t = 1 - T/T_2$. The open (solid) circles and triangles are for values of t with $T_2 = 57.94$ K (57.96 K). From the slope of the straight lines the exponent of $\alpha_2(E_{02})$ is $+0.50 \pm 0.03$ (-0.45 ± 0.03).

E_{0n} is shown. The data for both α_n and E_{0n} at the two transitions may be fitted to straight lines in the log-log plot against the reduced temperature $t = (T/T_n - 1)$. The slope of the straight lines passing through α_1 and α_2 (circles) is

$$\beta_1 = 0.50 \pm 0.07, \tag{5a}$$

$$\beta_2 = 0.50 \pm 0.03, \tag{5b}$$

where $\alpha_n \propto |t|^{\beta_n}$. In anticipation of the discussion which relates α_n to the order parameter the critical index of α_n has been identified[9] with β. The slope of the E_{0n} lines is -0.45 ± 0.05 (for E_{01}) and -0.45 ± 0.03 (for E_{02}). Due to the larger error bars in the E_{0n} data the case for a power-law behavior near T_n is less firmly established than for α_n. As is well known in the interpretation of such data the slope of the "best fit" is affected by the choice of the critical temperature T_n. In Fig. 3 the solid circles correspond to choosing T_2 as 57.96 K while the open circles correspond to $T_2 = 57.94$ K. How-

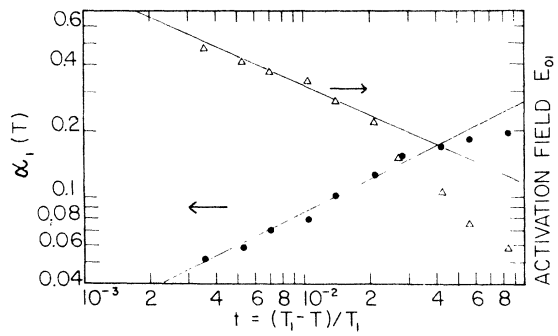

FIG. 4. Log-log plot of α_1 (circles) and E_{01} (triangles) versus the reduced temperature $t = 1 - T/T_1$. From the two lines the exponents for α_1 and E_{01} are $+0.50 \pm 0.07$ and -0.45 ± 0.05, respectively.

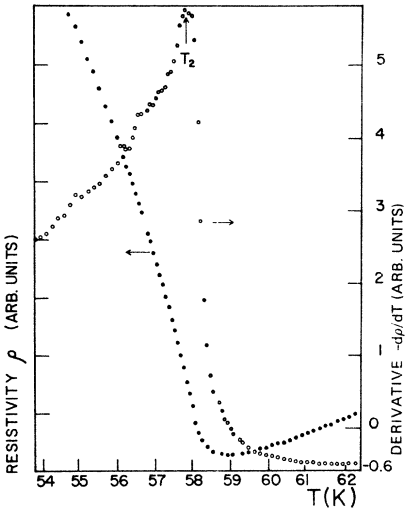

FIG. 5. Resistivity (solid circles) and its derivative with respect to temperature (open circles) near T_2. T_2 is taken to be where $d\rho/dT$ peaks.

ever, precision resistivity measurements[10] on the ferromagnetics near the Néel point have shown that the derivative of the resistivity is divergent at the Néel point. Recently, similar measurements[11,12] on the one-dimensional CDW metal tetrathiafulvalene-tetracyanoquinodimethane (TTF-TCNQ) and its selenium analog have shown the existence of a divergence in the derivative of the resistivity with respect to temperature. The transition temperature T_c in these systems is taken to be where the divergence occurs and it is found experimentally that the derivative of the resistivity behaves as a power law in the reduced temperature on either side of T_c. The critical index is different on both sides of the transition. As an aid to locating T_1 and T_2 in $NbSe_3$ the low-(electric)-field resistivity has been measured at 70 mK intervals near the two transitions. Figures 5 and 6 show for the T_2 and T_1 transitions the derivative

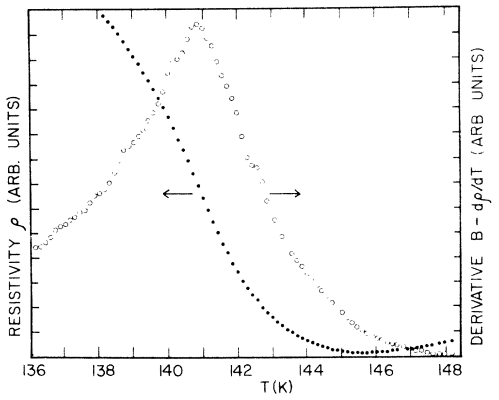

FIG. 6. Resistivity (solid circles) and its derivative with respect to temperature (open circles) near T_1.

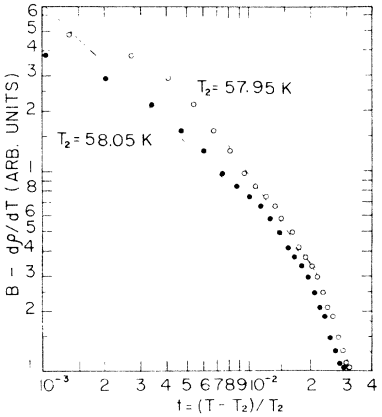

FIG. 7. Log-log plot of the derivative of the low-field resistivity (with background subtracted) vs the reduced temperature $t = (T - T_2)T_2$. The solid (open) circles correspond to choosing T_2 equal to 58.05 K (57.95 K). The slopes of the two lines are −1.0 and −1.5.

(open circles) after the subtraction of the flat pretransition background B. As may be seen, the derivative peaks at a temperature below where the derivative changes sign. In both figures the solid circles represent the low-field resistivity (with zero suppressed). Unfortunately, substantial rounding of the divergence occurs, especially at T_1, and it is not possible to ascertain the transition points to better than 0.1 K. For the T_2 transition the divergence is at 58.00 ± 0.05 K. Although this is consistent with the value of T_2 (57.96 K) used in

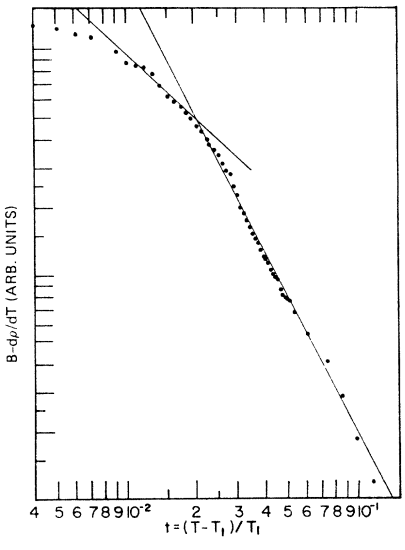

FIG. 8. Log-log plot of the derivative of the resistivity (with background subtracted) versus the reduced temperature near the T_1 transition. As discussed in the text the rounding of the divergence prevents an unambiguous measurement of the critical exponent near T_1. But at temperatures several K above T_1, the exponent is −2.0. This extends to about 15 K above T_1.

studying the critical behavior of α_2 the uncertainty of 100 mK prevents an unambiguous determination of the critical index of $d\rho/dT$. In Fig. 7 the derivative (after background subtraction) is plotted against the reduced temperature t in log-log scale. (The open circles are for $T_2 = 57.95$ K and the solid circles are for $T_2 = 58.05$ K.) The critical index lies between -1.0 and -1.5 depending on the choice of T_2. The flattening of the curves for $t < 3 \times 10^{-3}$ reflects the rounding off of the divergence. A similar situation obtains for the T_1 transition. The peak determined by the derivative data occurs at 141.0 ± 0.1 K. This is substantially lower than the value of 142 K used in the analysis of the critical behavior of α_1. This discrepancy is larger than the uncertainty in both measurements and is not understood. Figure 8 shows the log-log plot of the derivative versus t. As in Fig. 7 substantial rounding occurs near T_2 and it is not possible to extract a critical index in this region. However, for $t > 2 \times 10^{-2}$ the derivative obeys $d\rho/dT \propto t^{-2.0}$ over an interval of 15 K above T_1. The index is insensitive to any reasonable choice of T_1. This fluctuation contribution to the resistivity over such a wide range of temperature makes the T_1 transition appear much "broader" than the T_2 transition in the resistivity-temperature profile.

IV. THEORETICAL AND DISCUSSION

A. Charge-density-wave model

The arguments in favor of the CDW model in $NbSe_3$ have been reviewed in some detail in Ref. 3. Briefly, these are based on data from the pressure dependence[2] of T_1 and T_2, the detection of a heat-capacity anomaly[2] at T_2, the rapid rise of the superconducting transition temperature[13] T_c under pressure, and the extraction of the parameters[3] α_n which are consistent with gap formation at the FS. Recently, the Hall effect[7] and Young's modulus[14] have been measured. The Hall constant R_H shows an abrupt rise at both T_1 and T_2, indicating a decrease in carrier concentration at these transitions. The elastic modulus along the chain direction shows a small anomaly at T_1 (but none was detected at T_2). Both these experiments are consistent with the CDW model, since the Young-modulus measurement indicates a structural change (at least at T_1) while the Hall measurement provides direct evidence for a loss of carriers associated with these structural transitions. In the face of the accumulated indirect evidence it appears worthwhile to pursue the CDW hypothesis further even though more direct evidence (x-ray or neutron-scattering data) is not available.

We consider the Fröhlich electron-phonon (e-p) Hamiltonian

$$H = \sum_{\vec{k}} \epsilon_{\vec{k}} c_{\vec{k}}^{\dagger} c_{\vec{k}} + \sum_{\vec{q}} \hbar\omega_{\vec{q}} b_{\vec{q}}^{\dagger} b_{\vec{q}} + \frac{1}{\sqrt{N}} \sum_{\vec{k},\vec{q}} g_{\vec{q}} c_{\vec{k}+\vec{q}}^{\dagger} c_{\vec{q}} (b_{\vec{q}} + b_{-\vec{q}}^{\dagger}) , \tag{7}$$

where $c_{\vec{k}}^{\dagger}$ and $b_{\vec{q}}^{\dagger}$ are the creation operators for electrons and phonons, respectively, N is the number of ions, and $\omega_{\vec{q}}$ is the unrenormalized phonon frequencies. Within the random-phase approximation (RPA) the phonon frequencies will be renormalized[15] to

$$\Omega_{\vec{q}}^2 = \omega_{\vec{q}}^2 \left(1 + \frac{g_{\vec{q}}^2}{\hbar\omega_{\vec{q}} N} \sum_{\vec{k}} \frac{f(\epsilon_{\vec{k}}) - f(\epsilon_{\vec{k}-\vec{q}})}{\epsilon_{\vec{k}} - \epsilon_{\vec{k}-\vec{q}}}\right) . \tag{8}$$

In Eq. (8) the second term is proportional to the electronic susceptibility and $f(\epsilon_{\vec{k}})$ is the Fermi-Dirac distribution. Equation (8) may be derived by[15] computing the lowest-order contribution to the phonon self-energy and examining the pole of the phonon propagator computed within RPA. In most metals the correction is small except at $\vec{Q} = 2\vec{k}_F$ where the derivative of the correction with respect to q becomes infinite and Eq. (8) gives rise to the Kohn anomaly.[16] A much larger effect may arise in some systems if band pathologies allow the susceptibility to diverge for certain values of $\vec{q}$. As first pointed out by Lomer,[17] the existence of large portions of FS that are parallel (nest) would cause the denominator of the summand in Eq. (8) to vanish over a large fraction of phase space, for the value of $\vec{q}$ (called the spanning vector $\vec{Q}$) that brings about this nesting condition. This has been established as the mechanism which stabilizes spin-density wave[18] (SDW) state in Cr, and is also presumably the case in the layered compounds where CDW's occur.

The stability criterion may be taken as the condition $\Omega_{\vec{Q}} = 0$. From Eq. (8) this is equivalent to

$$1 + \frac{g_{\vec{Q}}^2}{\hbar\omega_{\vec{Q}} N} \sum_{\vec{k}} \frac{f(\epsilon_{\vec{k}}) - f(\epsilon_{\vec{k}-\vec{Q}})}{\epsilon_{\vec{k}} - \epsilon_{\vec{k}-\vec{Q}}} = 0 . \tag{9}$$

Extensive calculations on the SDW state exist in the literature. With a slight modification the results may be applied to CDW systems as well. From the paper by Fedders and Martin[19] (FM) the stability criterion for the SDW state is

$$1 + \frac{V(0)\gamma^2}{\Omega} \sum_{\vec{k}} \frac{f_a(\epsilon_{\vec{k}}) - f_b(\epsilon_{\vec{k}-\vec{Q}})}{E_a(\vec{k}) - E_b(\vec{k}-\vec{Q})} = 0 , \tag{10}$$

$$V(0) = 4\pi e^2/\mathcal{S}_{\mathrm{FT}}^2 , \tag{11}$$

where Ω is the volume, $V(0)$ is the long-wavelength screened Coulomb interaction, γ is a matrix element, e is the electronic charge, and $\mathcal{S}_{\mathrm{FT}}$ is the Fermi-Thomas screening length. The subscripts

a, b refer to the electron and hole bands, respectively. The occurrence of two (or more) types of carriers is indicated in $NbSe_3$ by the Hall effect[7] which reverses sign at 15 K. It is possible that nesting may occur between hole and electron pockets as in Cr. In any case, the results we shall use from the FM calculation will not be affected by this assumption. The energies measured from the FS are given by

$$\epsilon_a(k) = E_a(k) - E_F = v_a(k - k_c), \tag{12}$$

$$\epsilon_b(k) = E_b(k + Q) - E_F = v_b(k - k_c), \tag{13}$$

where v_a, v_b are velocities at the FS in the two bands and k_c is an average Fermi momentum. The FM results are analogous to those of the BCS theory[8] of superconductivity. They obtain for the transition temperature T_c,

$$k_B T_c = (2\gamma_e \bar{v}\bar{k}_c f/\pi) e^{-1/\lambda_{SDW}}, \tag{14}$$

where

$$\ln f = (K^2 + 2Kk_c - 6k_c^2)/4k_c^2, \tag{15}$$

$$\lambda_{SDW} = [\gamma^2 V(0) k_c^2/2\pi^2 v], \quad \ln\gamma_e = 0.577\ldots, \tag{16}$$

$$\bar{k}_c^2 = k_c(K - k_c), \quad \bar{v} = (v_a v_b)^{1/2}, \quad v = \tfrac{1}{2}(v_a + v_b). \tag{17}$$

The assumptions made in evaluating Eq. (10) are that the surfaces of constant energy in both bands are spherical and congruent. The first Brillouin zone has also been approximated by a sphere of radius K. FM also derive an equation for the gap function Δ. In the two limits $T \to 0$, $T \to T_c$, Δ is given by

$$\Delta(T \to 0) = \pi v k_B T_c/\gamma_e \bar{v} = 1.76(v/\bar{v}) k_B T_c, \tag{18}$$

$$\Delta(T \to T_c^-) = 3.06(v/\bar{v})(k_B T_c)(1 - T/T_c)^{1/2}. \tag{19}$$

The results in Eqs. (14)–(20) may be applied to a CDW system provided we change the coupling constant λ_{SDW}. Comparing Eqs. (9) and (10) we may define the equivalent coupling constant given by

$$\lambda_{CDW} = g_Q^2 \Omega k_c^2/\hbar\omega_Q N 2\pi^2 v. \tag{20}$$

In Eq. (19) the gap increases as $(1 - T/T_c)^{1/2}$ near T_c. This may also be derived from the Landau expansion[20] of the free energy

$$F_{CDW} - F_N = a\psi^2 + (\tfrac{1}{2}b)\psi^4, \quad \psi \propto \Delta, \quad a = a'(T - T_c). \tag{21}$$

Minimizing $(F_{CDW} - F_N)$ with respect to ψ we have

$$\Delta \propto \psi = [a'(T_c - T)/b]^{1/2}. \tag{22}$$

The specific-heat discontinuity is given by

$$C_V/\Omega = T_c a'^2/b = -2T_c(F_{CDW} - F_N)/(T_c - T)^2. \tag{23}$$

Using FM's result[19] for the decrease in the free energy near the transition

$$F_{CDW} - F_N = -(k_c^2 \bar{v}^2/4\pi^4 v^3 k_B^2 T_c^2)[\tfrac{7}{8}\zeta(3)]\Delta^4, \tag{24}$$

we have for the specific-heat discontinuity

$$C_v/\Omega = [4/7\zeta(3)](k_c^2 v/\bar{v}^2)(k_B^2 T_c). \tag{25}$$

B. α parameter and the energy gap

In $NbSe_3$ the non-Ohmic results reported here indicate a strong correlation between the behavior of α_n in Figs. 1 and 2 and the order parameter described by Eq. (22). In the following, arguments will be developed to establish the relationship of α with the gap Δ. Although the non-Ohmic behavior is still not understood it is possible to extract information on the FS by examining the $E = 0$ and $E = \infty$ limits of the conductivity. We make the assumption that the drop in conductivity at T_1 and T_2 is due to the loss of FS area which results from gap formation over the nesting fraction. Since the gap is very small for temperatures near T_c there will be substantial thermal excitation of carriers across the gap at these temperatures. As the gap increases, these excitations will drop rapidly in number. In the low E-field limit we may express the conductivity as[21] (suppressing the n subscript)

$$\sigma(E \to 0) = \sigma_N + \sigma_G 2f(\beta\Delta), \tag{26}$$

$$f(\beta\Delta) = (e^{\beta\Delta} + 1)^{-1}. \tag{27}$$

In Eq. (26), $\beta = (k_B T)^{-1}$, Δ is the gap size, and σ_N (σ_G) represents the conductivity associated with the FS area not affected by the gap (destroyed by the gap). Comparing Eq. (26) with Eq. (3) we have

$$\sigma_a = \sigma_N + 2f\sigma_G. \tag{28}$$

In the strong-field limit excitations induced by the infinite field saturate the non-Ohmic mechanism and we recover the pretransition behavior [obtained by setting $\Delta = 0$ in Eq. (26)]. From Eq. (4) we have

$$\sigma_a + \sigma_b = \sigma_N + \sigma_G. \tag{29}$$

Using Eqs. (28) and (29) in Eq. (2), α may be written

$$\alpha = [\sigma_G/(\sigma_N + \sigma_G)]\tanh(\tfrac{1}{2}\beta\Delta). \tag{30}$$

Insofar as σ_N and σ_G have the same temperature dependence, the coefficient of $\tanh(\frac{1}{2}\beta\Delta)$ in Eq. (30) will be only weakly temperature dependent. Near T_c we may expand [using Eq. (19)]

$$\alpha(T)/\alpha(0) \simeq \tfrac{1}{2}\beta_c\Delta \simeq 1.53(1 - T/T_c)^{1/2}(v/\bar{v}). \tag{31}$$

This accounts for the behavior of $\alpha(T)$ shown in Figs. 1–4. In Eq. (31), $\alpha(0)$ is the value of $\alpha(T)$ at $T = 0$ and $\beta_c = (kT_c)^{-1}$. Taking the experimental values appropriate to the T_2 transition

$$\alpha_2(0) = 0.63 \pm 0.01 \tag{32}$$

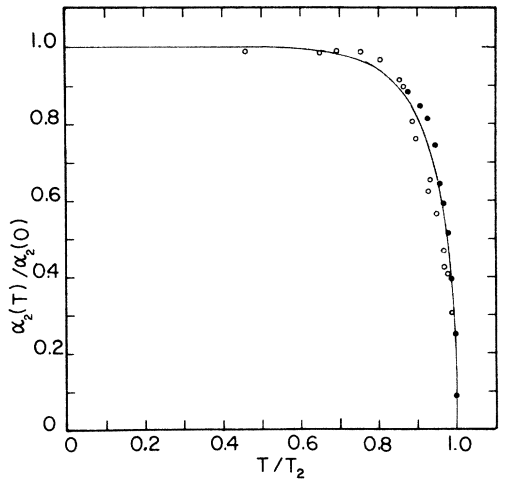

FIG. 9. Temperature dependence of $\alpha_2(T)/\alpha_2(0)$. The line is the theoretical expression $\tanh(\frac{1}{2}\beta\Delta)$ [see Eq. (30)] with $\Delta = 2.12\,\Delta_{BCS}$. The solid circles are the data from Fig. 1 while the open circles, which have more scatter, are from previously published measurements (Ref. 3) on another sample.

and

$$\alpha_2(T) = 2.05(1 - T/T_2)^{1/2}, \quad T \to T_2^-, \tag{33}$$

we have for $(v/\bar{v})_2$ the value [using Eq. (33) in Eq. (31)]

$$(v/\bar{v})_2 = 2.12 \pm 0.05. \tag{34}$$

Equation (34) expresses the ratio of the gap measured in $NbSe_3$ (at T_2) and the BCS gap. From Eqs. (18) and (34) we derive a theoretical value for the zero-temperature gap,

$$\Delta_2(0) = 3.73 k_B T_2 = 19 \text{ meV}. \tag{35}$$

At the T_1 transition the corresponding numbers are

$$(v/\bar{v})_1 = 2.8, \quad \Delta_1(0) = 60 \text{ meV}. \tag{36}$$

In Fig. 9 we compare the experimental data on α_2 with the BCS-FM model. The measured values of $\alpha_2(T)/\alpha_2(0)$ for two samples are compared with Eq. (30). The line is the theoretical curve $\tanh(\frac{1}{2}\beta\Delta)$. Values of Δ were obtained by multiplying the values of Δ_{BCS} provided by Mühlschlegel[22] by the scale factor $(v/\bar{v})_2$ given in Eq. (34). The solid circles are the data in Fig. 1 while the open circles which show more scatter are from earlier published results[3] on another sample.

The Landau-type mean-field theory predicts that the electronic specific heat shows a discontinuity at T_2 with a contribution given by Eq. (25). Although thermal measurements on $NbSe_3$ are sparse we may venture a comparison with the early results of Chaussy *et al.*[2] The specific heat shows a large anomaly (6×10^5 erg/cm^{3}K) at 52 K. This is to be compared with the 1.7×10^5 erg/cm^{3}K anomaly at the CDW transition[23] in $2H$-$NbSe_2$. Using Eq. (34) in Eq. (35) we compute a discontinuity in C_v/Ω of 9×10^3 (3×10^4) erg/cm^{3}K assuming a carrier density of 10^{20} cm^{-3} (10^{22} cm^{-3}), and an effective mass of 0.3 times the free-electron mass.[24] The electronic contribution is clearly too small to account for the large observed anomaly, and one has to include the lattice contribution. However, a large lattice contribution would appear to be inconsistent with the Young's modulus (ϵ) measurements[14] which detected no change in ϵ to 3 parts in 10^4 at T_2. More-accurate measurements of the heat capacity at both transitions are necessary before a realistic estimate of the electronic contribution can be made.

C. Activation field E_0 and nonlinear excitations

In many ways the non-Ohmicity of the conductivity below T_1 is the most interesting and puzzling property of $NbSe_3$. Efforts to interpret the observed behavior of σ given by Eq. (1) have not been successful. The activated form of σ strongly suggests an electric-field induced quantum tunneling process. However, the very small E-field values (0.1-1 V/cm) needed to induce non-Ohmicity have posed great difficulties in comparing theoretical expressions with experimental data. The simplest theory which reproduces Eq. (1) is that of Zener tunneling[4] across a gap at the FS. However, the magnitude of the gap arrived at using measured values of E_0 is two orders of magnitude smaller than $k_B T$. The E-field creation of soliton-antisoliton pairs in a one-dimensional CDW condensate has been discussed by Maki.[6] In this model the electric field induces a tunneling from a region in ϕ space (where ϕ is the CDW phase) to another region which corresponds to the appearance of a soliton-antisoliton pair. Interpreting Eq. (1) in terms of Maki's mechanism again leads to values of the soliton rest energy two orders of magnitude smaller than $k_B T$. Thus, the thermal creation of these solitons would appear to overwhelm the quantum creation at temperatures near T_1 and T_2. Recently, Larkin and Lee[25] (LL) have considered the problem of a one-dimensional CDW pinned by impurities, and the nonlinear conductivity arising from the quantum tunneling between impurity sites. In the strong pinning case they obtain for the non-Ohmic resistivity

$$\rho \propto \exp\{[2\pi v_F (m^*/m)^{1/2} \ln\epsilon\,]/eEl^2\}, \quad \epsilon = Vl/v_F, \tag{37}$$

where v_F is the characteristic velocity related to the elastic energy for deformation of ϕ, E is the electric field, V is the impurity strength, and l the

average distance between impurities. Applying their calculations to $NbSe_3$ LL conclude that the observed value of E_0 would require l to be extremely large. Furthermore, as in the previous two cases, thermal energy would dominate the energy supplied by the field. LL conclude that their impurity-pinning model is inapplicable to $NbSe_3$.

D. Critical divergence of $d\rho/dT$

The divergence of the derivative of the resistivity in pure metals and alloys at a phase transition appears to be very widespread. In ferromagnetics[10] such as Ni the derivative of ρ diverges logarithmically at the critical point T_N. In antiferromagnetic materials the divergence has a higher critical index). Fisher and Langer[26] (FL) have proposed that the divergence is due to critical scattering by the short-range spin fluctuations and have proposed a divergence $|t|^{-\alpha}$ (where α is the specific-heat index) above the Néel point T_N. Below T_N the scattering is dominated by the growing order parameter and $d\rho/dt \propto t^{2\beta-1}$ (where β is the order-parameter critical index). This agrees with what is experimentally observed in Ni. However, in antiferromagnetics the divergence above T_N has a higher critical index. Suezaki and Mori[27] (SM) have pointed out that the long-range spin fluctuations are dominant (above T_N) in the case of antiferromagnetics, where fluctuations occur around the wave vector $\vec{Q}$, leading to large angle scattering of conduction electrons. This is particularly true in SDW metals such as Cr where $\vec{Q} = 2\vec{k}_F$. The microscopic calculations of Takada[28] point to the same conclusion, namely, long-range fluctuations are dominant in antiferromagnetics while short-range fluctuations are dominant in ferromagnetics. Recently Horn and Guidotti[12] (HG) have studied the divergence of $d\rho/dT$ in the pseudo-one-dimensional organic metals [TTF-TCNQ and tetraselenafulvalene-tetracyanoquinodimethane (TSeF-TCNQ)] at the Peierls transition T_P. They found that (above T_P) the critical index is -1.0 along both axes in TTF-TCNQ and -1.5 along the b axis in TSeF-TCNQ. These indices are substantially larger than those found in the magnetic materials (0.0 to -0.3). To explain their results they considered the effect on $d\rho/dT$ of restricting the allowed final states for scattering due to the reduced dimensionality d of the metal. Using mean-field values for the critical exponents HG obtain the results[27]

$$\frac{d\rho}{dT} \propto \begin{cases} t^{-1.5} & (d=1), \\ t^{-1.0} & (d=2), \\ t^{-0.5} & (d=3). \end{cases} \tag{38}$$

The derivative of the resistivity arising from the long-range fluctuations may be written as [cf. Eq. (3.9) of Ref. 27]

$$\frac{d\rho_{\mu T}}{dT} \propto Q_\mu Q_\tau g_{\vec{Q}}^2 \sum_{\vec{q}} f_{\vec{q}}(1 - f_{\vec{Q}+\vec{q}}) \times \mathrm{Re} \int_0^\infty dt \exp(-i\omega_{\vec{Q}+\vec{q},\vec{q}} t - \Gamma t) \times \sum_{\vec{k}} \Psi_{\vec{Q}+\vec{k}}(t), \tag{39}$$

where $\vec{Q}$ is the spanning vector of the CDW, $g_{\vec{Q}}$ is the electron-phonon coupling constant, $f_{\vec{q}}$ is the Fermi-Dirac distribution, Γ^{-1} is the lifetime of the electrons, and

$$\Psi_{\vec{K}}(t) = -\frac{\partial \chi_{\vec{K}}(t)}{\partial T}. \tag{40}$$

In Eq. (40), $\chi_{\vec{K}}$ is the density-density correlation function which diverges at $T = T_c$ for $\vec{K} = \vec{Q}$. To evaluate Eq. (39) the assumption of critical slowing down is made so that we may neglect[27] the time dependence of $\Psi_{\vec{k}}$ in Eq. (40) and it is valid to use the static scaling laws,[9]

$$\chi_{\vec{Q}+\vec{k}}(0) = t^{-\gamma} F(k/\kappa). \tag{41}$$

In Eq. (41), γ is the susceptibility critical index, F is an unknown function, and κ is the inverse correlation length which behaves as (for $T \to T_c$)

$$\kappa \propto t^{\nu}. \tag{42}$$

The dimensionality d of the electron gas enters when we evaluate $\sum_{\vec{k}} \Psi_{\vec{Q}+\vec{k}}$. Using Eqs. (41) in Eq. (40) and performing the sum over $\vec{k}$ we have

$$\sum_{\vec{k}} \Psi_{\vec{Q}+\vec{k}}(0) \propto t^{-\gamma-1} \kappa^d \int_0^\infty dx\, x^d G(x). \tag{43}$$

Substituting Eq. (43) in Eq. (39) we finally have [using Eq. (42)]

$$\frac{d\rho_{\mu T}}{dT} \propto Q_\mu Q_\tau t^{-\gamma-1+\nu d}. \tag{44}$$

Using mean-field values ($\gamma = 1$, $\nu = \frac{1}{2}$) we have HG's results [Eq. (38)].

In $NbSe_3$ the critical exponent lies between -1 and -1.5 at the T_2 transition. Using the above theory this implies that the dimensionality of the system is 2 or 1, the data being insufficiently unambiguous to decide between the two. However, a value of -0.5 or smaller for the critical exponent can be excluded rather definitely. At the T_1 transition the rounding of the divergence very near T_1 prevents an extraction of the index. For $t > 2 \times 10^{-2}$, however, an exponent of 2 is obtained. This is larger than the result in Eq. (44) using reasonable values of γ, ν, and d. It is possible that the assumptions underlying the derivation of Eq. (44) no longer hold at temperatures well above T_1. In particular the

critical slowing-down assumption is expected to be invalid far above T_1 and one needs to examine the dynamics of the fluctuations without this simplifying assumption.

V. SUMMARY AND CONCLUSION

The non-Ohmic conductivity of $NbSe_3$ has been measured at temperatures in the vicinity of the two phase transitions at T_1 and T_2. At each temperature the conductivity may be decomposed into a field-independent part σ_a and a field-dependent part $\sigma_b e^{-E_0/E}$ (suppressing the subscript n, which identifies the transition). From σ_a and σ_b a parameter α is obtained which (at $T = 0$ K) gives the fraction of FS affected by the gap. (In a multiband model the pockets of FS which do not participate in the CDW formation are included in σ_a.) At elevated temperatures (particularly a few K below T_1 and T_2) thermal excitations across the growing gap reduce the value of α from its $T = 0$ K value. Therefore the temperature dependence of α provides information on the temperature dependence of the gap. By applying Fedders and Martin's theory to a CDW system we have theoretically computed the temperature variation of α using a BCS-type gap. Good agreement between the calculations and the data is obtained. This agreement may be interpreted as new evidence for gap formation at the FS at both transitions. The loss of carriers due to gap formation has also been observed directly in recent Hall measurements. From the fit of α to the BCS gap theoretical values for the zero temperature gaps have been calculated. The magnitude is 60 meV (19 meV) for the gap corresponding to the T_1 (T_2) transition. The transport measurements reported here also provide some information on the dimensionality of the electronic band-structure. By studying the divergence of the resistivity derivative at T_2 we conclude that the dimensionality is less than three. In conjunction with the large Hall effect and strong galvanomagnetic response at low temperatures, and the absence of a metal-to-insulator (Peierls) transition we believe that the dimensionality is closer to two than to one.

Although some progress has been made in interpreting the non-Ohmic data the actual mechanism for the striking electric breakdown of the anomalies remains a puzzle. A number of theories based on quantum tunneling are successful in explaining the electric-field dependence of the conductivity, but numerical comparison with the experimental data seems to come up against the paradoxical situation that the energy supplied by the electric field is much smaller than the thermal fluctuation energy at T_1 and T_2.

Note added in proof. Electron diffraction evidence of superlattice formation in $NbSe_3$ at T_1 has been reported by Tsutsumi, Takagaki, Yamamoto, Shiozaki, Ido, Sambongi, Yamaya, and Abe, Phys. Rev. Lett. 39, 1675 (1977). X-ray diffraction evidence for a new superlattice at T_2 has also been obtained by Fleming and co-workers [P. A. Lee (private communication)]. Ayrolles and Roucan have also observed the superlattice at T_1 by electron diffraction . [P. Monceau (private communication)].

ACKNOWLEDGMENTS

Illuminating and encouraging discussions with K. Maki and P. Kumar are gratefully acknowledged. The author would like to thank P. Horn for suggesting the critical-divergence measurements and P. Monceau for early communication of results. The sample preparation by J. Savage has been indispensable to the work reported here. This work was supported by the Office of Naval Research Grant No. N00014-77-C-0473.

[1] A. Meerschaut and J. Rouxel, J. Less-Common Metals 39, 197 (1975).
[2] J. Chaussy, P. Haen, J. C. Lasjaunais, P. Monceau, G. Waysand, A. Waintal, A. Meerschaut, P. Moninie, and J. Rouxel, Solid State Commun. 20, 759 (1976).
[3] N. P. Ong and P. Monceau, Phys. Rev. B 16, 3443 (1977).
[4] P. Monceau, N. P. Ong, A. M. Portis, A. Meerschaut, and J. Rouxel, Phys. Rev. Lett. 37, 602 (1976).
[5] M. J. Rice, A. R. Bishop, J. A. Krumhansl, and S. E. Trullinger, Phys. Rev. Lett. 36, 432 (1976).
[6] K. Maki, Phys. Rev. Lett. 39, 46 (1977).
[7] N. P. Ong and P. Monceau, Solid State Commun. (to be published).
[8] J. Bardeen, L. N. Cooper, and J. R. Schrieffer, Phys. Rev. 108, 1175 (1957).
[9] L. P. Kadanoff, W. Götze, D. Hamblen, R. Hecht, E. A. S. Lewis, V. V. Palciauskas, M. Rayl, J. Swift, D. Aspnes and J. Kane, Rev. Mod. Phys. 39, 395 (1967).
[10] P. P. Craig, W. I. Goldburg, T. A. Kitchens, and J. I. Budnick, Phys. Rev. Lett. 19, 1334 (1967).
[11] P. M. Horn and D. Rimai, Phys. Rev. Lett. 36, 809 (1976).
[12] P. M. Horn and D. Guidotti, Phys. Rev. B 16, 491 (1977).
[13] P. Monceau, J. Peyrard, J. Richard, and P. Molinie, Phys. Rev. Lett. 39, 160 (1977).
[14] J. W. Brill and N. P. Ong, Solid State Commun. (to be published).
[15] See, for example, A. L. Fetter and J. D. Walecka, *Quantum Theory of Many-Particle Systems* (McGraw-Hill, New York, 1971), p. 411.
[16] W. Kohn, Phys. Rev. Lett. 2, 393 (1959).
[17] W. M. Lomer, Proc. Phys. Soc. Lond. 80, 489 (1962).
[18] See, for example, C. Herring, in *Magnetism*, edited by G. T. Rado and H. Suhl (Academic, New York, 1966), Vol. IV. See also, S. K. Chan and V. Heine, J. Phys. F 3, 795 (1973).

[19]P. A. Fedders and P. C. Martin, Phys. Rev. 143, 245 (1965).
[20]See Ref. 15, p. 430.
[21]I am indebted to K. Maki for suggesting this analysis.
[22]B. Mühlschlegel, Z. Phys. 155, 313 (1959).
[23]J. M. E. Harper, T. H. Geballe, and F. J. DiSalvo, Phys. Lett. A 54, 27 (1975).
[24]This is the value of the carrier mass observed by Shubnikov–de Haas oscillation measurements. P. Monceau, Solid State Commun. 24, 331 (1977).
[25]A. Larkin and P. A. Lee, Phys. Rev. B 17, 1596 (1978).
[26]M. E. Fisher and J. S. Langer, Phys. Rev. Lett. 20, 665 (1968).
[27]Y. Suezaki and H. Mori, Prog. Theor. Phys. 41, 1177 (1969).
[28]S. Takada, Prog. Theor. Phys. 46, 15 (1971).